



Supplementary Information for

**Widespread organ tolerance to Xist loss and X reactivation except under chronic stress in the gut**

Lin Yang<sup>1,2</sup>, Eda Yildirim<sup>1,2†</sup>, James E. Kirby<sup>3</sup>, William Press<sup>1,2</sup>, and Jeannie T. Lee<sup>1,2\*</sup>

<sup>1</sup> Department of Molecular Biology, Massachusetts General Hospital, Boston, MA USA

<sup>2</sup> Department of Genetics, The Blavatnik Institute, Harvard Medical School, Boston, MA USA

<sup>3</sup> Department of Pathology, Beth Israel Deaconess Medical Center, Harvard Medical School, Boston, MA 02114, USA

† Current address: Department of Cell Biology, Duke University School of Medicine, Duke Cancer Institute, Durham, NC 27710

Corresponding author: Jeannie T. Lee

**Email:** [lee@molbio.mgh.harvard.edu](mailto:lee@molbio.mgh.harvard.edu)

**This PDF file includes:**

Figures S1 to S6

Tables S1 to S4

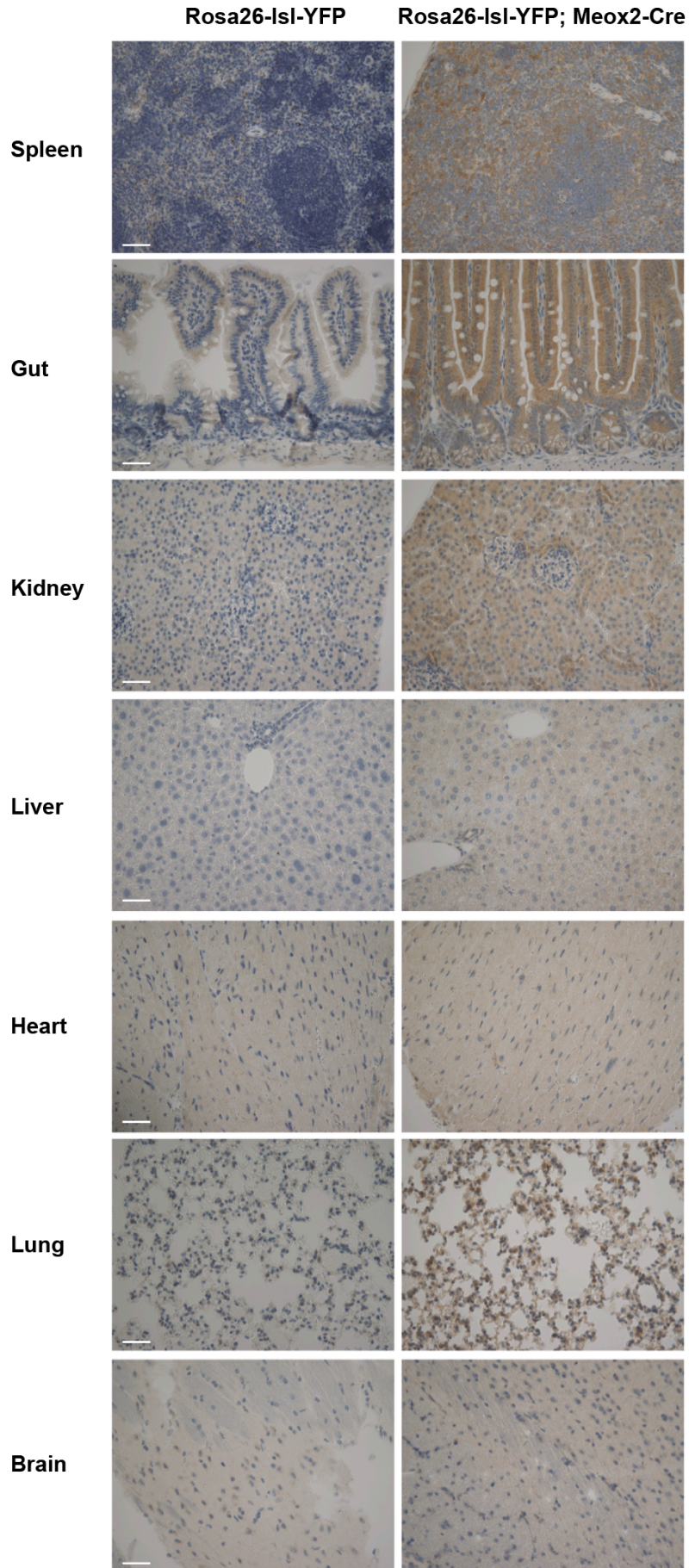


**Fig. S1. Meox2-Cre is highly active in multiple tissues.** Meox2-Cre activity assessed by expression of YFP following excision of the lox-stop-lox (Isl). Immunostaining for YFP (brown) in multiple tissues as indicated.

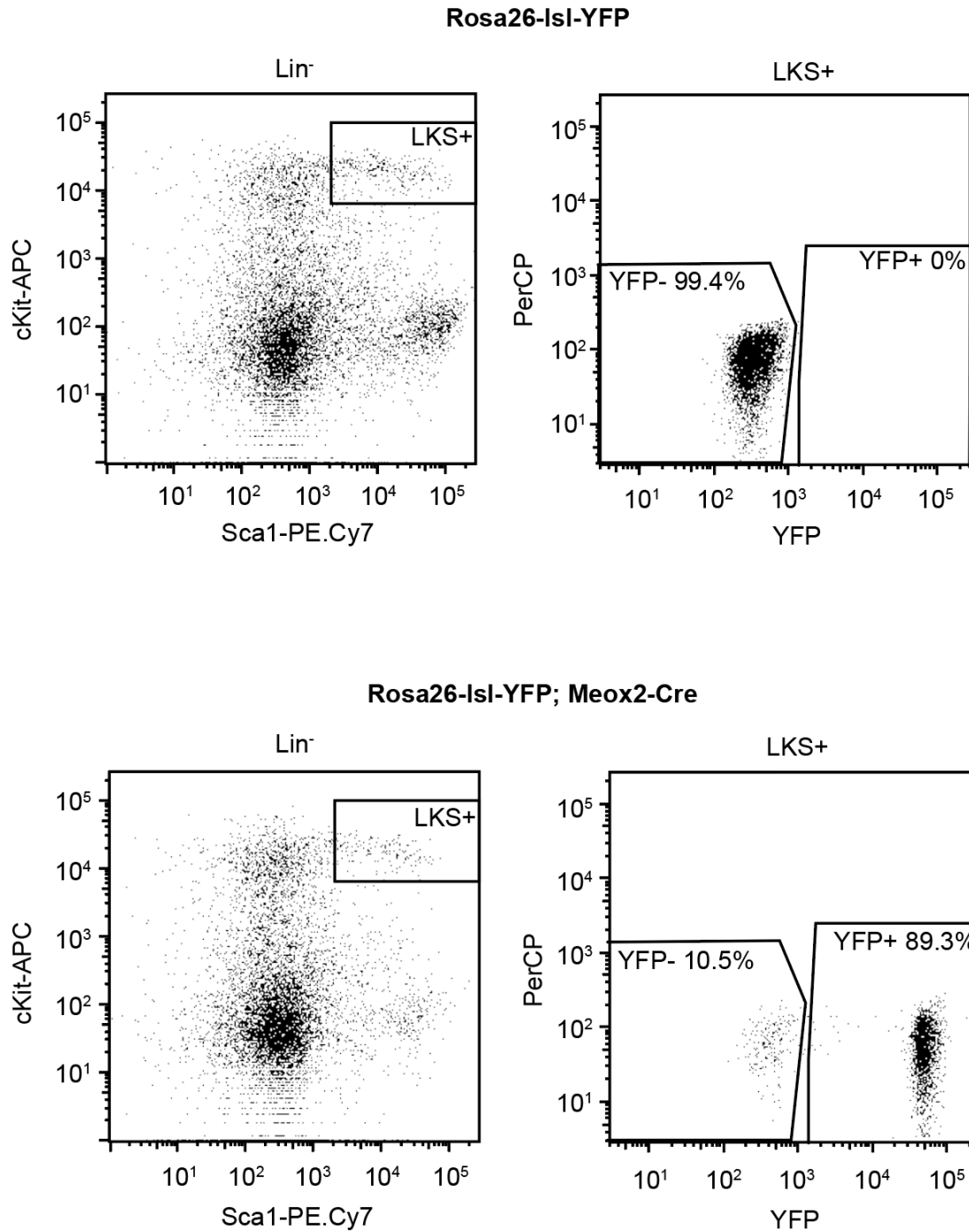


**Fig. S2. Meox2-Cre is highly active in blood.** Quantification of YFP<sup>+</sup> cells amongst LKS<sup>+</sup> (Lineage<sup>-</sup> cKit<sup>+</sup> Sca1<sup>+</sup>) cells by FACS analysis. Top panel, Rosa26-IsI-YFP control animals; bottom panel, Rosa26-IsI-YFP; Meox2-Cre animals.



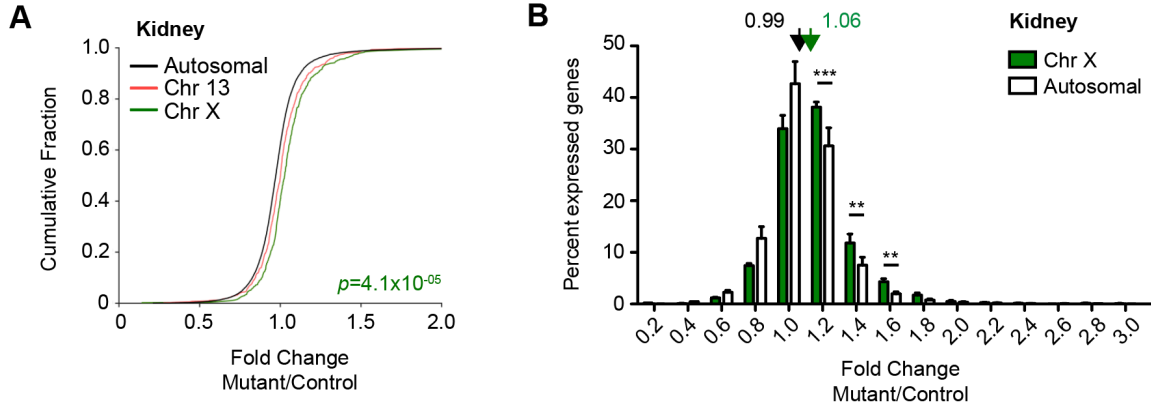


**Fig. S3. *Xist*-deleted organ of *Meox2*-Cre females show mild X-autosome dosage imbalance.**

(A) Cumulative frequency plot for fold changes of genes on chromosome 13 (red), chromosome X (green) and all autosomes (black). Combined data for 3 biological replicates shown.  $p$ -value, Wilcoxon's rank-sum test. (B) Distribution of X-linked (green) versus autosomal (white) fold changes in three *Xist*-null kidneys relative to three controls. Average fold changes of X-linked or autosomal genes from three biological replicates are indicated. \*\*  $p < 0.01$ ; \*\*\*  $p < 10^{-8}$ , Fisher's exact test. Data represents mean  $\pm$  SEM.

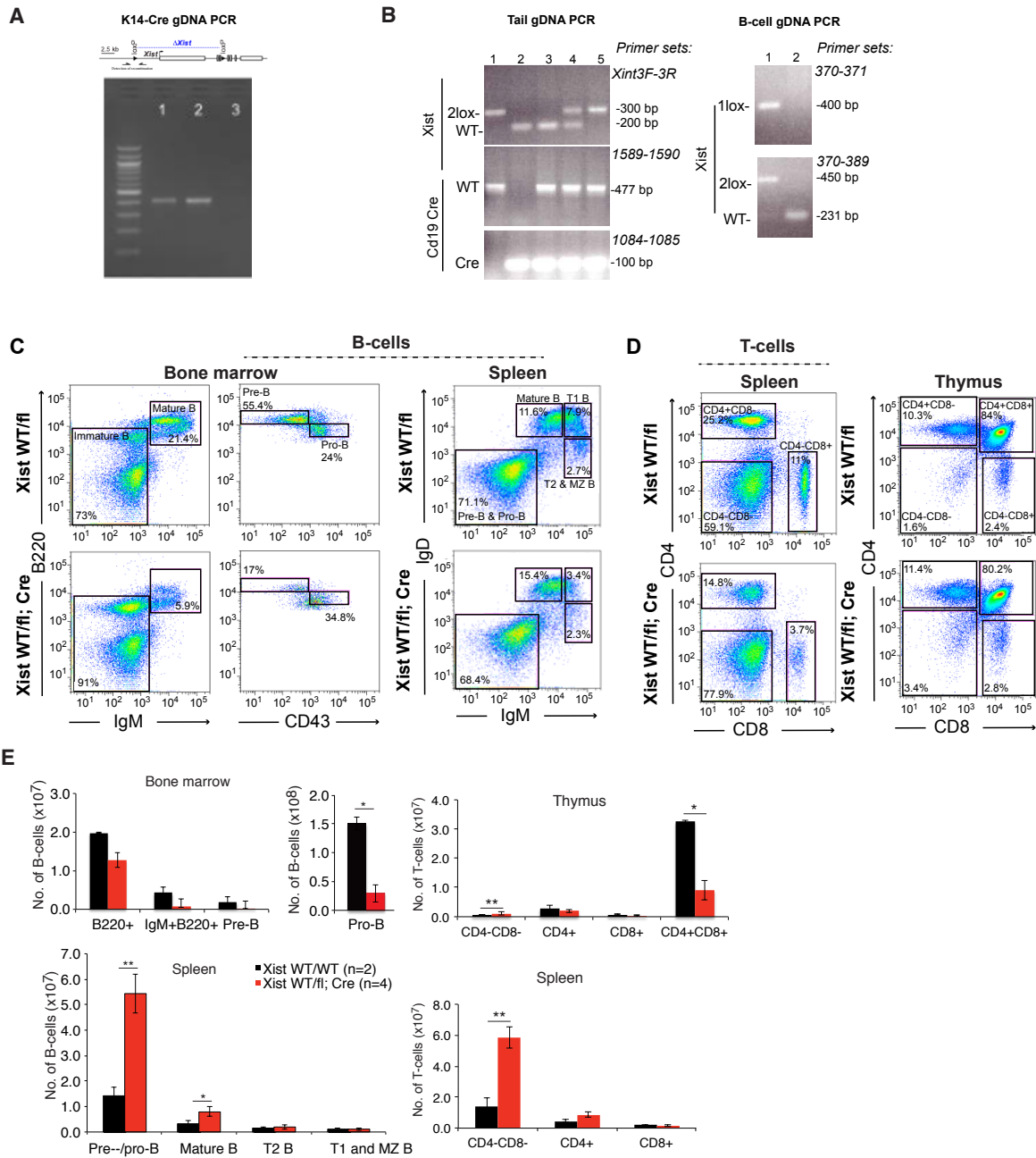


**Fig. S4.** Recombination efficiencies for Keratin14-Cre and CD19-Cre mutants with **FACS analysis** of CD19-cre-deleted *Xist* females.

(A) Genomic DNA of *Xist*<sup>fl/fl</sup>; Keratin14-Cre animals was isolated from: (1) dorsal skin epidermis, (2) tail epidermis and (3) the spleen. Primer set for detection of recombination across the loxP site was used for PCR genotyping. (B) Genotyping of genomic DNA (gDNA) from tail (left) and B cells (right)

isolated from  $Xist^{WT/fi};CD19\text{-cre}$  mouse cohort. (Left) Tail gDNA samples represent the following genotypes (1)  $Xist^{fi/fi};CD19\ +/+$ , (2)  $Xist^{WT/WT};CD19\ cre/cre$ , (3)  $Xist^{WT/WT};\ CD19\ cre/+$ , (4)  $Xist^{fi/WT};\ CD19\ cre/+$ , (5)  $Xist^{fi/fi};\ CD19\ cre/+$ . (Right) B cell gDNA samples represent the following genotypes (1)  $Xist^{fi/fi};\ CD19\ cre/+$ , (2)  $Xist^{WT/WT};CD19\ +/+$ . (C-E) FACs analyses of B and T cell numbers in bone marrow, thymus, and spleen, as indicated, of  $Xist^{WT/fi}$  versus  $Xist^{WT/fi};\ CD19\text{-cre}$  females. (C, D) Original FACs data. (E) Percentages plotted in graphs, shown as means  $\pm$  SEM. Significance is calculated using t-test. \* $p<0.05$ ; \*\* $p<0.01$ .

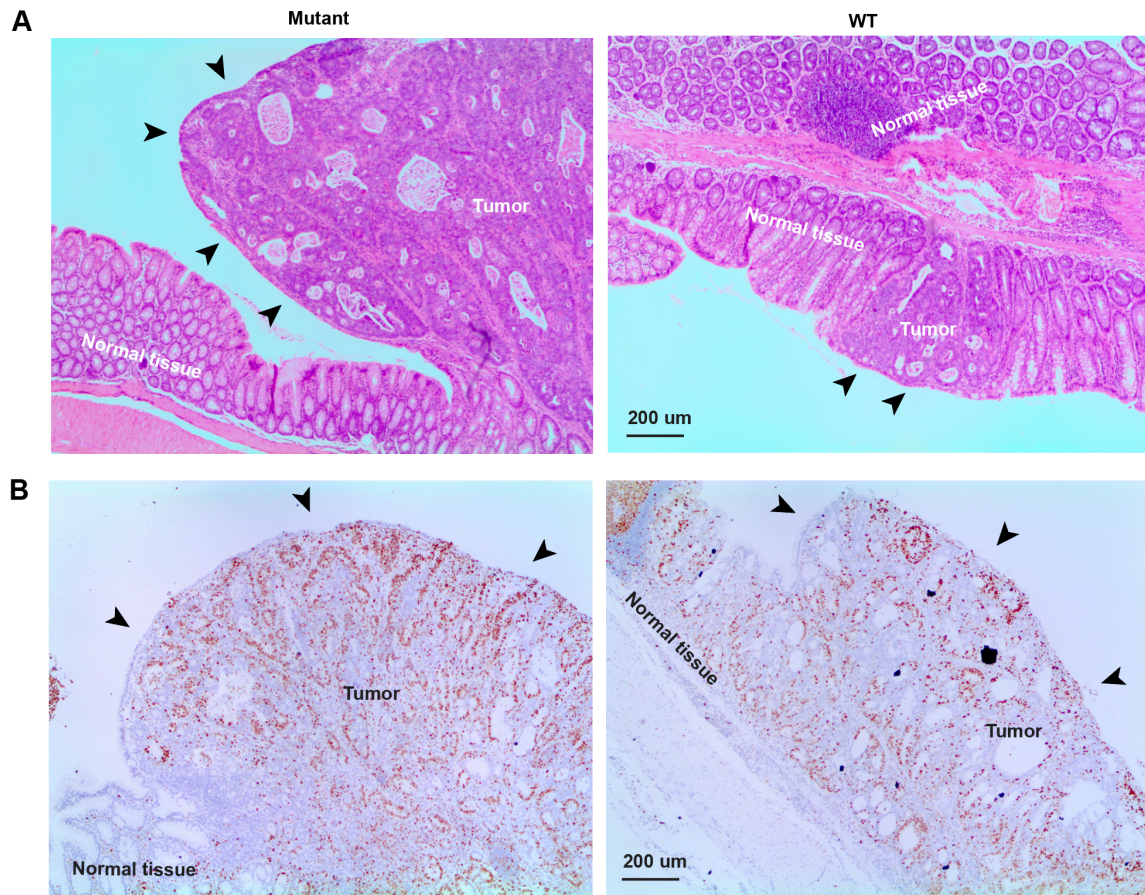


**Fig. S5. Histologic analysis of mutant and control guts following AOM/DSS induction.** (A) 40x magnifications of a single polyp/tumor in mutant versus control mice. H&E stained. (B) 40x magnification of immunohistochemical staining for the cell proliferation marker, Ki67 (brown), in mutant and control gut sections. Arrowheads point to polyps.

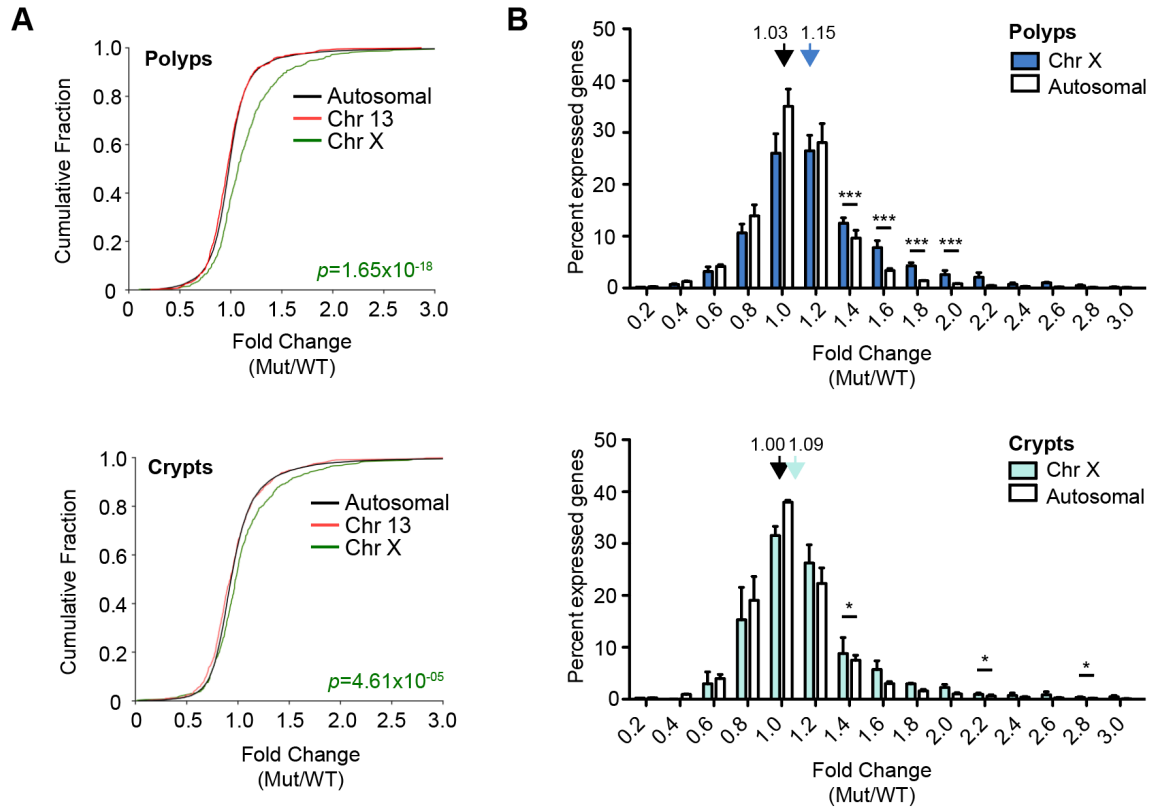


**Fig. S6. Supplemental transcriptomic analysis of crypts and polyps in *Xist*-deleted and control gut.**

(A) Cumulative frequency plots for fold changes of genes on chromosome 13 (red), chromosome X (green) and all autosomes (black). Combined data for the biological replicates shown in Figures 6 and 7.  $p$ -value, Wilcoxon's rank-sum test. (B) Distribution of X-linked (blue, polyps; cyan, crypts) versus autosomal (white) fold changes in *Xist*-null polyps/crypts relative to corresponding controls. Combined data for the biological replicates shown in Figures 6 and 7. \*  $p < 0.05$ ; \*\*  $p < 0.01$ ; \*\*\*  $p < 10^{-8}$ , Fisher's exact test. Data represents mean  $\pm$  SEM,  $n=2$  (crypts),  $n=4$  (polyps).